Resource allocation in networks via coalitional games

Shams, F.

Citation

Shams, F. (2016, September 21). *Resource allocation in networks via coalitional games*. Retrieved from https://hdl.handle.net/1887/45667

Version:	Not Applicable (or Unknown)
License:	Licence agreement concerning inclusion of doctoral thesis in the Institutional Repository of the University of Leiden
Downloaded from:	https://hdl.handle.net/1887/45667

Note: To cite this publication please use the final published version (if applicable).

Cover Page

Universiteit Leiden

Leiden University Repository

The handle http://hdl.handle.net/1887/45667 holds various files of this Leiden University dissertation.

Author: Shams, F.
Title: Resource allocation in networks via coalitional games
Issue Date: 2016-09-21

Chapter 3

A resource allocation cooperative game in OFDMA

Following what discussed in Chapter 2, various attempts have been made to standardize a certain protocol for resource allocation in OFDMA, but all have fallen into disuse largely because of their over-complexity, and unfairness from the network service provider point of view. We also showed that cooperative game theory is a suitable tool to face resource allocation problems, especially when altruism and fairness play crucial roles.

The focus of the first part of this thesis is to introduce a scheme for resource allocation in OFDMA based on cooperative games, wherein applicability and fairness are target criterions. This chapter investigates a fair adaptive resource management criterion for the uplink of an OFDMA network populated by mobile users with constraints in terms of target data rates. We aim at fulfilling each users QoS requirement in terms of target transmit rates *exactly* with the best utilization of the network resources, so as to satisfy both the users and the wireless service provider. We also aim at designing a low-complexity algorithm that allows a centralized solution for the joint power and bandwidth allocation for OFDMA uplink channels to be achieved in a few steps using typical network parameters. In our approach, we allow every subcarrier to be possibly *shared* among more than one user, and we add a constraint on the maximum number of used subcarriers per terminal. This is achieved by dividing the available bandwidth into a number of disjoint blocks of consecutive subcarriers, and forcing each terminal to use at most one subcarrier per block. The motivation of this is twofold: we wish to *i*) increase the signal-to-interference-plus-noise ratio (SINR) on the used subcarriers, which also simplifies channel estimation; and *ii*) exploit frequency diversity across carriers used by one user to increase the performance of forward error correction (FEC) techniques.

In Sect. 3.1 we propose two methods to allot subcarriers to mobile terminals, in a possibly shared assignment. Next, the inherent optimization problem is tackled with the analytical tools of cooperative game theory aiming at accomplishment of data rate demanded exactly. The definition of the players, coalitions and utility function are formally discussed, and we prove the existence of the core set solution by means of the analytical tools of cooperative game theory. To accomplish data rate demanded we propose a utility function which is neither convex nor concave. Sect. 3.2 proposes a dynamic learning algorithm based on Markov modeling to achieve optimum transmit power over each subcarrier at each individual wireless terminal. Simulation results in Sect. 3.3 show that the average number of operations of the proposed algorithm is much lower than $K \cdot N$, where N and K are the number of subcarriers and users. We also show that the transmit power is comparable to the remarkable existing power effective literature results. Low-complexity, efficient use of available spectrum, and low power consumption bring promise to usability of the proposed scheme in each time slot at physical layer in the 4G of cellular networks.

3.1 Problem formulation

Let us consider the uplink of a single-cell infrastructure OFDMA system with total bandwidth W, subdivided in N subcarriers with frequency spacing $\Delta f = W/N$. The cell is populated by K mobile terminals, each terminal $k \in \mathcal{K} = [1, \ldots, K]$ experiencing a complex-valued channel gain H_{kn} on the nth subcarrier to the base station and having a data rate requirement $R_k^\star$ (in bit/s). We assume that fulfilling such constraints simultaneously by all terminals is feasible. To exploit frequency diversity, the subcarriers set $\mathcal{N} = [1, \ldots, N]$ is grouped in B blocks of N/B contiguous subcarriers $\mathcal{N}^{(b)} = \left[\frac{N}{B}(b-1)+1, \ldots, \frac{N}{B}b\right] \subset \mathcal{N}$, with $1 \leq b \leq B$, as shown in Fig. 3.1. Each terminal is allowed to take at most one subcarrier per each subblock.

Our resource allocation strategy consists in finding a vector of transmit powers $\mathbf{p}_k$, where $\mathbf{p}_k = \left[p_{k1}, \ldots, p_{kN}\right]$, with p_{kn} representing the power allocated by terminal k over its nth subcarrier, that allows the QoS constraint $R_k^\star$ to be satisfied. We decouple the problem into the subsequential resolution of subchannel assignment and (subsequent) power allocation.

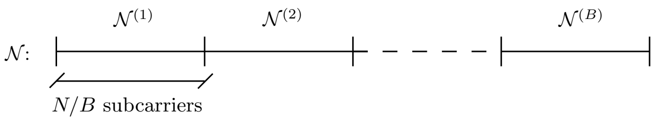

Fig. 3.1: *Block partitioning of the available bandwidth.*

3.1.1 Subchannel assignment

We describe here two different options to perform this function:

Best-carrier assignment

For every subblock $\mathcal{N}^{(b)}$, every terminal $k \in \mathcal{K}$ is assigned its best subcarrier $n_k^{(b)} = \arg\max_{n \in \mathcal{N}^{(b)}} |H_{kn}|^2$. The probability of assigning the same subcarrier to multiple mobile terminals is non-null.

Vacant-carrier assignment

In a sequential manner, for every subblock $\mathcal{N}^{(b)}$, every terminal $k \in \mathcal{K}$ is assigned its best subcarrier $n_k^{(b)} = \arg\max_{n \in \mathcal{N}^{(b)}} |H_{kn}|^2$. But, if $k \leq N/B$, we would like to ensure exclusive use of each subcarrier $n \in \mathcal{N}^{(b)}$ to better exploit the available bandwidth W (i.e., to reduce the multiple access interference). So, if $n_k^{(b)}$ has been already assigned to some other terminal $\ell < k$, then terminal k is assigned the nearest vacant (unassigned) subcarrier to $n_k^{(b)}$ within the channel coherence bandwidth. Clearly, this is not considered if $k > N/B$, so that terminal k is assigned its best subcarrier in the subblock anyway. Note that the ordering of $\mathcal{K}$ has a negligible impact on system performance when N is sufficiently high and, as usual, $N \gg K$ (e.g., 2048 subcarriers in LTE).

Both assignment strategies can be easily extended to the case in which each terminal is allowed to have a different number of assigned subcarriers (different B for each mobile terminal), based on its own data rate requirement $R_k^\star$, without any change in the strategy that we describe below. For the sake of simplicity, we consider the same B for all terminals.

3.1.2 Power allocation

To derive a stable solution to the power allocation subproblem, we consider it as a coalitional game, in which each subchannel $n_k^{(b)} \in \mathcal{N}$ is identified as a player in the game. To model the coalitional game, we build K coalitions $\psi = [\mathcal{A}_1, \ldots, \mathcal{A}_K]$, to be assigned to the K terminals. Each coalition $\mathcal{A}_k$, $k \in \mathcal{K}$, contains the B players $n_k^{(b)}$: $\mathcal{A}_k = \left[n_k^{(1)}, \ldots, n_k^{(B)}\right]$. Note that i) the members of each coalition are fixed, since one player cannot move from one coalition to another; and ii) since a subcarrier $n \in \mathcal{N}$ can be shared among multiple users, there exist virtual copies of it belonging to different coalitions. For the sake of notation, we will identify with a generic $n \in \mathcal{A}_k$ any of the subcarriers assigned to terminal k. The strategy of each player $n \in \mathcal{A}_k$ is represented by the optimal power expenditure $p_{kn} \leq \overline{p}_{kn}$. Note that i) if $n \notin \mathcal{A}_k$, $p_{kn} = 0$; and ii) if $n \in \mathcal{A}_k$, we can also have $p_{kn} = 0$, which means that the kth terminal does not transmit on the nth subcarrier, and it thus bears an actual number of active subcarriers $B'_k < B$.

The system under investigation aims at fulfilling the QoS requirement of every terminal k in terms of target rate $R_k^\star$. For simplicity, we estimate the achieved data rate as the Shannon capacity R_k of terminal k, that can be approached by using suitable channel coding techniques [283]:

$$R_k = \sum_{n \in \mathcal{N}} R_{kn} \tag{3.1}$$

where R_{kn} is the Shannon capacity achieved by terminal k on subcarrier n:

$$R_{kn} = \Delta f \cdot \log_2 \left(1 + \frac{|H_{kn}|^2 \, p_{kn}}{\sum_{m \neq k} |H_{mn}|^2 \, p_{mn} + \sigma_w^2} \right). \tag{3.2}$$

Clearly, $R_{kn} = 0$ if $n \notin \mathcal{A}_k$, since $p_{kn} = 0$. If $n \in \mathcal{A}_k$, R_{kn} depends on the received SINR at the base station on subcarrier n, which is a function of the strategy (i.e., the transmit power) chosen by player n (i.e., one of the B subcarriers assigned to the kth terminal), of the transmit power of other terminals on the same subcarrier (if $n \notin \mathcal{A}_m$, $p_{mn} = 0$), of the corresponding channel gains, and of the power of the additive white Gaussian noise (AWGN) σ_w^2. Note that, in an OFDMA system, there is no interference between adjacent subcarriers. Hence, R_{kn} considers only intra-subcarrier noise, that occurs when the same subcarrier is shared by more terminals. Each player $n \in \mathcal{A}_k$ causes interference only to its virtual copies, i.e. to the players of other coalitions such that $n_m^{(b')} = n \in \mathcal{A}_m$, with $m \neq k$ and for any b', $1 \leq b' \leq B$.

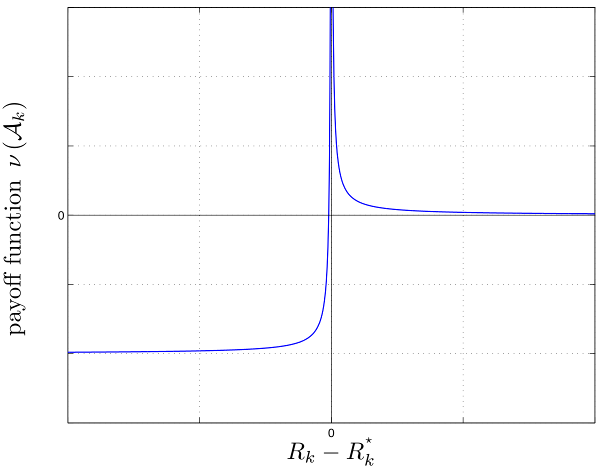

Fig. 3.2: *Shape of the utility as a function of the Shannon capacity.*

The network service provider are satisfied at most when each mobile terminal k achieves its own data rate requirement *exactly*: $R_k = R_k^\star$. In view of this goal, we can force all players in each coalition $\mathcal{A}_k$ to select their strategies (i.e., the power allocation for terminal k over the available bandwidth W) so as to maximize a utility function for the kth coalition $\mathcal{A}_k$, defined as:

$$\nu(\mathcal{A}_k) = \frac{1}{|R_k/R_k^\star - 1|} - \beta \cdot \mathrm{u}\left(1 - R_k/R_k^\star\right) \tag{3.3}$$

where $\mathrm{u}(\cdot)$ is the unit step function, with $\mathrm{u}(y) = 1$ if $y \geq 0$ and $\mathrm{u}(y) = 0$ otherwise (see Fig. 3.2).

If $R_k = R_k^\star$, $\mathcal{A}_k$ earns the highest possible payoff $\nu(\mathcal{A}_k) = +\infty$. If $R_k > R_k^\star$, $\mathcal{A}_k$ gets a positive payoff, whereas it obtains a negative payoff if $R_k < R_k^\star$. The factor β is a positive constant (much) greater than zero that ensures $\nu(\mathcal{A}_k)$ to be negative when $R_k < R_k^\star$. This is expedient to let the players distinguish a capacity R_k that is lower/upper than $R_k^\star$ only by knowing their own coalition's payoff. Note that, in practice, $+\infty$ can be represented by the largest countable number available (e.g., $2^{64} - 1$) in a given computational platform.

The payoff of each coalition is a real number and, in our formulation, the most important parameter is the gain of each coalition, whereas the outcome of each player does not matter at all. Therefore, this game is a transferable utility (TU) one [10,22].

The specific shape of our utility function (3.3) is actually immaterial, and was chosen to ensure fast convergence of the iterative algorithm that will be introduced later on. We could have considered any utility function which increases as its argument moves from $\pm\infty$ to 0, just to make sure that, for any $R_k \neq R_k^\star$, each coalition has an incentive to move towards $R_k = R_k^\star$.

To provide further insight into the problem, we investigate now some properties of the proposed game $\mathcal{G}$. As a first step, we note that the players in $\mathcal{G} = (\mathcal{K} = \bigcup_{k\in\mathcal{K}} \mathcal{A}_k, \nu)$ with the utility function (3.3), do *not* tend to form the grand coalition. This is because every player $n \in \mathcal{A}_k$ can not leave its coalition $\mathcal{A}_k$: the members of each coalition are fixed and do not change during the game. This may appear inappropriate to the notion of a coalitional game. However, our assumption is fairly common in economic problems like the study of a bargaining game between two corporations when each corporation has its own business branches [284]. In this case the members (branches) of each coalition (corporation) are fixed.

A relevant result for our game is the following:

Theorem 3 *The core of the game $\mathcal{G} = (\mathcal{K} = \bigcup_{k\in\mathcal{K}} \mathcal{A}_k, \nu)$ with utility function (3.3) is not empty.*

Proof The number of coalitions and the number of players in each coalition are both fixed. Since each player belongs just to one coalition, the unique balanced collection of weights $(\mu_\mathcal{A})_{\mathcal{A}\in\psi}$ is $\mu_\mathcal{A} = 1 \;\; \forall\, \mathcal{A} \in \psi$. To conclude the proof, we must verify that $\sum_{\mathcal{A}\in\psi} \nu\,(\mathcal{A}) \leq \max_{\psi\in\boldsymbol{\Psi}} \sum_{\mathcal{A}\in\psi} \nu\,(\mathcal{A})$. Since the target rates of all terminals are assumed to be feasible, then every coalition expects R_k to approach $R_k^\star$. Therefore, every coalition is allowed to earn the highest possible payoff. ■

In the following section, we will show how the fundamental properties of our game lead to a practical allocation algorithm.

3.2 The best-response algorithm

We are interested in answering questions like: *How do the players set their proper transmit powers?* Dynamic learning models provide a framework for analyzing the way the players may set their proper strategies. A player adopts a certain power amount if and only if this matches its coalition's interests, and this goal can be achieved through a best-response iterative algorithm [285] based on Markov modeling [286]. Each player takes its own decisions individually, myopically, and concurrently with the others, so as to lead its own coalition's payoff toward $+\infty$ ($R_k = R_k^\star$). At each (discrete) time step of the algorithm, the (autonomous) players simultaneously adjust their transmit powers based on a model to increase the payoff of their own coalitions. Although this leads to interference when virtual copies of the same subcarriers simultaneously change their powers, we show that this dynamic myopic procedure guarantees the maximum payoff to each coalition.

The process starts up at time step $t = 0$ with an arbitrary assignment of the transmit powers $p_{kn}^{t=0}$ to all $K \cdot B$ players in the game (that are grouped in K coalitions with players $n \in \mathcal{A}_k$ with $n = n_k^{(b)}$, $1 \leq b \leq B$). At the generic time step t, our system is in the state $\omega^t = (\psi^t, \boldsymbol{\nu}^t)$, where ψ^t is the set $[\mathcal{A}_1^t, \ldots, \mathcal{A}_K^t]$, and $\boldsymbol{\nu}^t = [\nu(\mathcal{A}_1^t), \ldots, \nu(\mathcal{A}_K^t)] \in \mathbb{R}^K$ contains the payoffs of the coalitions in ψ^t. The evolution of the Markov chain is then dictated by the strategy of the game. The strategy of each player $n \in \mathcal{A}_k$ is to find the best power amount p_{kn}^t that leads to an increase in the payoff $\nu(\mathcal{A}_k^t)$ of its own coalition $\mathcal{A}_k$. In practice, player $n \in \mathcal{A}_k$ decides whether to change its power allocation, making its coalition better off, or to keep transmitting at the same power level (e.g., when its coalition's payoff is infinite). The following pseudocode shows how each player $n \in \mathcal{A}_k$ takes its decision at time step t:

if $\nu(\mathcal{A}_k^t) = +\infty$, then $p_{kn}^{t+1} = p_{kn}^t$, exit;
else *//setting correct power range*
  if $\nu(\mathcal{A}_k^t) \leq 0$, then $\tilde{p}_{kn} = p_{kn}^t$, $\tilde{p}_{kn}^{\max} = \overline{p}_{kn}$;
          else $\tilde{p}_{kn} = 0$, $\tilde{p}_{kn}^{\max} = p_{kn}^t$;
repeat
  $\hat{p}_{kn} = \tilde{p}_{kn}$; *//saving tentative power*
  compute $\nu(\tilde{\mathcal{A}}_k)$; *//tentative payoff*
  $\Delta\tilde{p}_{kn} = \texttt{unif}\left[0, \overline{\Delta p}_{kn}\right]$; *//random power step*
  $\tilde{p}_{kn} = \tilde{p}_{kn} + \Delta\tilde{p}_{kn}$; *//tentative power*
until $(\nu(\tilde{\mathcal{A}}_k) > \nu(\mathcal{A}_k^t))$ or $(\tilde{p}_{kn} > \tilde{p}_{kn}^{\max})$
if $(\nu(\tilde{\mathcal{A}}_k) > \nu(\mathcal{A}_k^t))$, then $p_{kn}^{t+1} = \hat{p}_{kn}$; *//accept*
          else $p_{kn}^{t+1} = p_{kn}^t$; *//discard*

In this algorithm, $\nu(\tilde{\mathcal{A}}_k)$ is the "trial" value of the current payoff of the coalition when the tentative power $\tilde{p}_{kn}$ is adopted: it is computed with $p_{mn} = p^t_{mn}$ for all $n \in \mathcal{N}$ and for any $m \neq k$, and $p_{kn} = \tilde{p}_{kn}$. At each step of the update process, the power step $\Delta\tilde{p}_{kn}$ is the particular outcome (value) of a random variable uniformly distributed between 0 and $\overline{\Delta p}_{kn}$, with $\overline{\Delta p}_{kn} \ll \overline{p}_{kn}$. As better detailed in Sect. 3.3, optimal values for $\overline{\Delta p}_{kn}$ can be found in order to minimize the algorithm computational load, based on experimental results. If $\nu\left(\mathcal{A}^t_k\right) \leq 0$, then $R_k < R^\star_k$, and the best strategy for player $n \in \mathcal{A}_k$ is to increase its current transmit power so as to increase its coalition's payoff. As a result of the random power stepping, the tentative power is a random number in the interval $[p^t_{kn}, \overline{p}_{kn}]$. Player $n \in \mathcal{A}_k$ accepts this value if and only if the coalition payoff $\nu\left(\mathcal{A}^t_k\right)$ increases, otherwise it ends up transmitting at its previous value. If $0 < \nu\left(\mathcal{A}^t_k\right) < \infty$, player $n \in \mathcal{A}_k$'s best strategy is on the contrary to decrease p^t_{kn}, and thus the tentative (random) transmit power belongs to the interval $[0, p^t_{kn}]$. At the end of each time step t, the base station computes the payoff $\nu\left(\mathcal{A}_k\right), \forall k \in \mathcal{K}$ with updated power amounts. As shown in the pseudocode, a uniformly distributed random power stepping is adopted to increase the probability of picking the best adjustment value, and thus both to reduce the convergence time of the algorithm and to possibly minimize the overall power consumption. As is apparent, the convergence speed of the algorithms depends not only on the parameters of the network, but also on the choice of the maximum update step $\overline{\Delta p}_{kn}$.

As already stated, two copies $n \in \mathcal{A}_k$ and $n \in \mathcal{A}_m$ (the virtual copies of the same subcarrier n) may happen to wish to adjust their transmit powers in a conflicting (and thus incompatible) way. If we assume that each player just follows the decision rules listed in the pseudocode above, then the probability of conflicting decisions will be high. To reduce the occurrence of this event, we modify our algorithm by requesting each player *not* to update its transmit power at every step of the game with a probability $\lambda \in [0, 1]$. At each time step t, every player $n \in \mathcal{A}_k$ selects a random number ξ^t_{kn} uniformly distributed in $[0, 1]$. If $\xi^t_{kn} > \lambda$, then the player applies the algorithm and (possibly) update p^{t+1}_{kn}, otherwise $p^{t+1}_{kn} = p^t_{kn}$ (i.e., during time step t, it skips the update process, and the value of p^t_{kn} is kept). If λ is close to 1, then the probability of conflicting decisions tends to 0, but the algorithm will have a large convergence time, since the probability of updates is low. In addition to the conflicts described above, another potentially disruptive condition may arise between different subcarriers belonging to the same coalition: if both (myopic) players simultaneously increase their powers $p^t_{kn} > 0$ and $p^t_{kn'} > 0$, it may occur that $R_k > R^\star_k$. To optimize the update mechanism and to cope with both negative kinds of events, we could consider a variable and adaptive threshold λ_{kn}^t for each virtual copy of the same subcarrier (each player). However, to reduce the complexity of the algorithm, we assume $\lambda_{kn}^t = \lambda > 0$ for all the players (i.e., virtual copies of the subcarriers). As better detailed in Sect. 3.3, the optimal value of λ must be selected as a suited trade-off. Note that the value of λ is common knowledge among the players at every step of the algorithm. Nevertheless, interference between concurrent, conflicting decisions may prevent the coalitions from achieving the expected payoff. If all coalitions earn less than the previous time step, all players assign the previous power amount for the next time step. There may exist network configurations in which the iterative algorithm is not guaranteed to converge. To account for these situations, we place a maximum number of operations Θ, beyond which the algorithm is stopped, and the sum of the users demands is thus labeled as unfeasible.

We show now that our proposed algorithm reaches a stable state at which no player attempts to change its own transmit power. Moreover we show that the stable state corresponds to the core apportionment of the game. We model the evolution of the algorithm as the output of a finite-state Markov chain with state space $\Omega = \{\omega = (\psi, \boldsymbol{\nu}) | \psi \in \boldsymbol{\Psi}, \boldsymbol{\nu} \in \mathbb{R}^K\}$. For all time steps t, $\psi^t = \psi$ belongs to the subset of all possible disjoint coalitions $\boldsymbol{\Psi}$ with exactly B members, and remains fixed for the whole duration of the algorithm. The time evolution of the algorithm as a Markov chain is due to the time variability of $\boldsymbol{\nu}^t$, which depends on the power levels p_{kn}^t chosen by the players in the coalitions collected by ψ^t. We use this notation for the sake of convenience, to emphasize that $\boldsymbol{\nu}^t$ is directly connected to ψ^t.

The Markov process asymptotically tends towards a stable coalition structure state, where no player has any incentive to change its power. In other words, all coalitions get their maximum payoffs. Our algorithm guarantees that, when $t \to \infty$, this Markov chain tends towards a singleton steady state with probability 1.

Definition 20 ([286]) *A set $\Phi \subset \Omega$ is an* ergodic set *if, for any $\omega \in \Phi$ and $\omega' \notin \Phi$, the probability of reaching the state ω' starting from ω is zero. Once the Markov chain falls into a state belonging to an ergodic set, it never leaves that set, and it wavers between the states in that ergodic set from then on. The probability of reaching any state in the ergodic set is strictly positive.*

Lemma 4 ([286]) *In any finite Markov chain, no matter which state the process* *starts from, the probability of ending up into an ergodic set tends to* 1 *as time tends to infinity.*

Definition 21 ([286]) *Singleton ergodic sets are called* absorbing states.

If Φ is an absorbing state and $\omega \in \Phi$, the probability of ending up into state ω when beginning from ω is one. In fact, absorbing states individually represent points of equilibrium.

Lemma 5 *The state* $\omega = (\psi, \boldsymbol{\nu})$ *is an absorbing state of the best-response process if and only if*

$$\nu\left(\mathcal{A}_k\right) = +\infty \quad \forall \mathcal{A}_k \in \psi \tag{3.4}$$

Proof This condition ensures that no player has any incentive to change its power amount. If this condition is met, then no coalition can get a higher payoff by deviating from state $\omega = (\psi, \boldsymbol{\nu})$. Since all the target rates are feasible, this condition is also necessary. ■

Theorem 4 *The best-response process has at least one absorbing state.*

Proof Since the best-response algorithm is a Markov process, Lemma 4 ensures that the best-response process reaches an ergodic set Φ. To conclude the proof, it is enough to show that Φ is singleton. Suppose that the number of states in the ergodic set is $|\Phi| > 1$. Then all players revise their strategies without conflicting decisions with a non-null probability. As a consequence, the Markov process moves to a new state, in which all coalitions' payoff are higher than those achieved in the previous state. This means that the probability of going back to the previous state is null, which contradicts the notion of an ergodic set. ■

Note that Theorem 4 does not ensure the uniqueness of the ergodic set in the best-response process. There may exist some different combinations of the power allocation for the players to reach to a steady state. It means that the game possesses multiple equilibria. The major finding of Theorem 4 is that, according to the way the players adjust their strategies, the best-response process leads to one of the steady states, in which no player has any incentive to revise its power allocation.

Theorem 5 *The set of payoffs associated to an absorbing state of the best-response process coincides with the set of core allocation:*

i) if $\omega = (\psi, \boldsymbol{\nu})$ is an absorbing state, then $\boldsymbol{\nu}$ is a core allocation.

ii) if $\boldsymbol{\nu}$ is a core allocation, then all $\omega = (\psi, \boldsymbol{\nu})$ are absorbing states.

Proof Part i) Suppose $\omega = (\psi, \boldsymbol{\nu})$ is an absorbing state but $\boldsymbol{\nu}$ is not a core allocation. In this case, there exist some coalitions that can obtain a higher payoff. This is contradictory, since the game reaches an absorbing state when every coalition gets the maximum payoff.

Part ii) If $\boldsymbol{\nu}$ is a core allocation, then no coalition can earn by letting its member change their powers. This implies that the state will not move to a new state, and thus the current state is absorbing. ■

Coalitional games aim at identifying the best coalitions of the agents and a fair distribution of the payoff among the agents. Interestingly, in this game the absorbing state coincides with one of the Nash equilibria [10] of the game. Suppose there are $K = 2$ mobiles connected to a base station with $N = 1$ subcarrier only. In this case, the $K = K \cdot N = 2$ copies of the subcarrier, each constituting a coalition, are engaged in a 2×2 game. Every player has two strategies: either $p_k = 0$ or $p_k = \overline{p}_k$. It is straightforward to verify that, in this game, a mixed (vs. pure) Nash equilibrium exists which satisfies the stability of the static game. With due attention to the notation, we can extend this result to a general case.

Theorem 6 *The set of absorbing states in the best-response process and the set of Nash equilibria of the static game are asymptotically (in the long run) equivalent.*

Proof Let us consider the coalitions in the best-response process as players in a static game. Lemma 4 ensures that this process reaches an ergodic set in the long run. According to Theorem 4, this set is singleton, and thus its member is an absorbing state. Hence, no coalition (i.e., no player in the static game) has any incentive to revise its strategy. In static games, this is the definition of a Nash equilibrium. ■

We can now conclude that the absorbing state is an extension of the Nash equilibrium, since the coalitions bind agreements with each other as economic agents and earn a vector value rather than a real number. Once the coalitions reach the absorbing state, their payoff is the highest possible ($+\infty$), and no coalition is willing to revise its current strategy. In general, as follows from Theorem 6, the Nash equilibrium of the game is Pareto-optimal (efficient), since no other strategy can achieve a payoff greater than $+\infty$.

3.3 Numerical results

In this section, we evaluate the performance of the best-response algorithm presented in Sect. 3.2. We consider some cases with different numbers of mobile terminals, target data rates, and subcarriers, showing that our suggested scheme reaches a steady state after a few steps only. To increase the convergence speed of the algorithm, we introduce a tolerance parameter ε in our utility function, such that, if $\left|R_k/R_k^\star - 1\right| < \varepsilon$, then we assume that the payoff is $+\infty$. We can possibly set an asymmetric range $[\varepsilon_1, \varepsilon_2]$ such that $\varepsilon_1 \leq (R_k/R_k^\star - 1) \leq \varepsilon_2$, so as to favor solutions with $R_k > R_k^\star$.

We consider the following parameters for our simulations: the maximum power of each terminal k on each subcarrier n is $\overline{p}_{kn} = \overline{p} = 3\,\mu\text{W}$; the power of the ambient AWGN noise on each subcarrier is $\sigma_w^2 = 100\,\text{nW}$, and the constant number in (3.3) is $\beta = 5000$. We also set $\Theta = 10K \cdot N$ as the stopping criterion of the iterative algorithm, where K and N depend on the network parameters of the simulation. The path coefficients $|H_{kn}|^2$, corresponding to the frequency response of the multipath wireless channel at the carrier frequency $n\Delta f$, are computed using the 24-tap ITU modified vehicular-B channel model adopted by the IEEE 802.16m standard [68]. To account for the large-scale path loss, we assumed the terminals to be uniformly distributed between 3 and 100 m. Based on numerical optimizations, the parameter λ that reduces the probability of conflicting decisions among members of different coalitions for different number of terminals, subcarriers, and signal bandwidth, is $\lambda = 0.97$. The initial power allocation is $p_{kn} = 0\ \forall k \in \mathcal{K}$ and $\forall n \in \mathcal{N}$. This experimentally provides the minimal power consumption at the steady state, and in most cases the minimum number of steps of the algorithm.

Fig. 3.3 reports the behavior of the achievable rate R_k as a function of the time step t in a network with $K = 10$ terminals, $N = 1024$ subcarriers, and bandwidth $W = 10\,\text{MHz}$ using the vacant-carrier assignment scheme. The target rates, reported in Fig. 3.3 with solid markers on the right axis, are assigned randomly to each terminal using a uniform distribution in the range $[100, 250]\,\text{kb/s}$. Further parameters are:

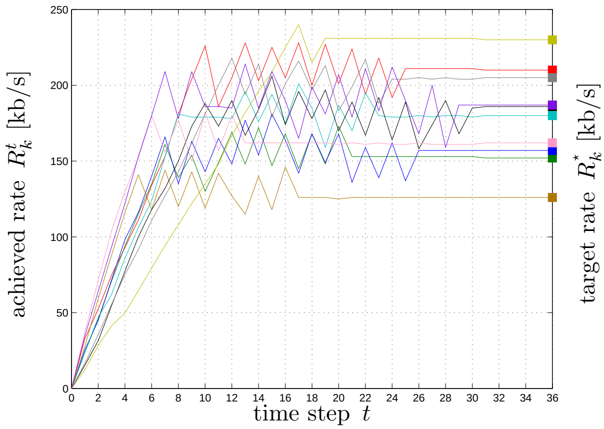

Fig. 3.3: *Achieved rates as functions of the iteration step.*

tolerance $\varepsilon_1 = 0, \varepsilon_2 = 0.01$, power update step $\overline{\Delta p}_{kn} = \overline{p}_{kn}/25 = 120\,\mathrm{nW}$, and number of subblocks $B = 32$. Numerical results show the convergence of R_k to the respective target rates $R_k^\star$ after 31 steps of the best-response algorithm.

In the remainder of this section, we will evaluate by simulation the average performance of our proposed algorithm in terms of power expenditure and computational burden using realistic system parameters and extensive simulation campaigns. Note that we are not able to compare our technique with the joint resource allocation techniques available in the literature and reviewed in Chapter 2.4, mainly due to the unfeasible algorithmic complexity of the implementation of the latter when using tens of terminals, hundreds of subcarriers, and high data rates (on the order of Mb/s). As a consequence, in the following we will compare our measured results with the theoretical performance provided by the literature.

Figs. 3.4 and 3.5 report the simulation results obtained after 500 random realizations of a network with $R_k^\star = R^\star = 200\,\mathrm{kb/s}$ $\forall k \in \mathcal{K}$, $N = 1024$, $W = 10\,\mathrm{MHz}$, and $\varepsilon_1 = 0, \varepsilon_2 = 0.04$ again with the vacant-carrier assignment strategy. Solid lines represent the case $\overline{\Delta p}_{kn} = \overline{p}_{kn}/5 = 600\,\mathrm{nW}$, whereas dashed lines depict the case $\overline{\Delta p}_{kn} = \overline{p}_{kn}/25 = 120\,\mathrm{nW}$. Circles, squares, upper triangles and lower triangles correspond to $B = \{8, 16, 32, 64\}$, respectively.

Fig. 3.4 shows the average normalized power expenditure ζ_k at the steady state as a function of K, computed by averaging $\zeta_k = \frac{1}{N}\sum_{n\in\mathcal{N}} \frac{p_{kn}}{\overline{p}_{kn}}$ over all terminals.

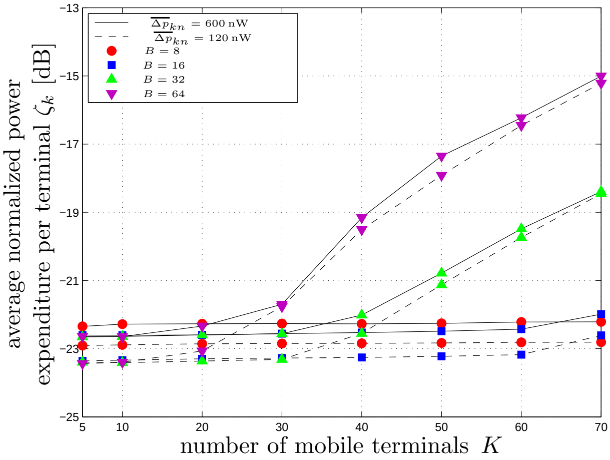

Fig. 3.4: *Average normalized power expenditure as a function of K, with $W = 10\,\mathrm{MHz}$, $N = 1024$, and $R_k^\star = R^\star = 200\,\mathrm{kb/s}$ $\forall k \in \mathcal{K}$ in the case of vacant-carrier assignment model.*

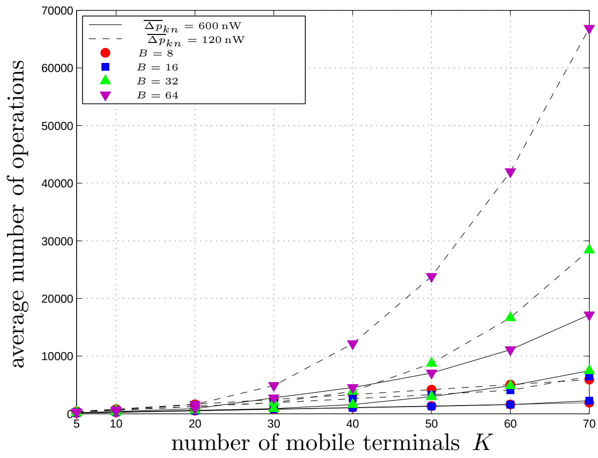

Fig. 3.5: *Experimental average number of operations as a function of K, with $W = 10\,\mathrm{MHz}$, $N = 1024$, and $R_k^\star = R^\star = 200\,\mathrm{kb/s}$ $\forall k \in \mathcal{K}$ in the case of vacant-carrier assignment model.*

This serves as a measure for the average total power consumption normalized to the maximum power expenditure available to each terminal. As can be noticed, ζ_k increases for $K \geq N/B$, since the number of shared subcarriers increases and the terminals must spend more power to overcome the intra-subcarrier noise. Interestingly, the power expenditure of the proposed centralized algorithm shows higher efficiency than the distributed and cross-layer schemes available in the literature (e.g., see [16, 17, 287, 288]). For instance, when considering 500 random realizations of a system with bandwidth $W = 10\,\text{MHz}$ and $N = 1024$ subcarriers, and using the vacant-carrier assignment model, we find that, in the case of a total sum-rate demand of 20 Mb/s (i.e., with a spectral efficiency of 2 b/s/Hz) and $R_k^\star = R^\star = 200\,\text{kb/s}$ (i.e., $K = 100$ terminals), the maximum power consumption per user is $31\,\mu\text{W}$ and the average power consumption of the system is 0.53 mW. In the multicell scenario of [16], the average power expenditure for each cell is 8 mW when the achievable data rate is 40 Mb/s. When considering the cross-layer algorithm proposed in [17], the average power expenditure per mobile terminal is 0.4 W with maximal spectral efficiency of 2 b/s/Hz, whereas the average power expenditure per mobile terminal required by the energy-efficient techniques proposed in [288] is 0.4 and 1.2 W when the achieved data rate is equal to 40 and 140 kb/s, respectively.

Fig. 3.5 shows the computational complexity of our algorithm expressed in terms of the average number of operations per terminal required to reach the steady state as a function of the number of terminals K with the vacant-carrier assignment model. The number of operations is measured experimentally by counting the number of steps required by the subchannel assignment plus the total number of trials required to update the transmit power according to the best-response algorithm. As can be seen, the complexity increases as B increases. This can be justified since increasing B increases the number of players $K \cdot B$, which yields an increase in the number of conflicting decisions. Note that the proposed algorithm is able to provide a spectral efficiency higher than 1 b/s/Hz, which occurs, for instance, when we assume more than $K = 50$ users with rates $R_k^\star = 200\,\text{kb/s}$ over a bandwidth $W = 10\,\text{MHz}$ in the proposed scenario, with a linear computational burden at the base station using appropriate values for the parameters. In this particular example, a good tradeoff between performance and complexity is $B = \{8, 16\}$ and $\overline{\Delta p_{kn}} = 600\,\text{nW}$. Using these values, the number of operations of the proposed algorithm is experimentally *lower* than the product $K \cdot N$, and so considerably *lower* than the complexity of

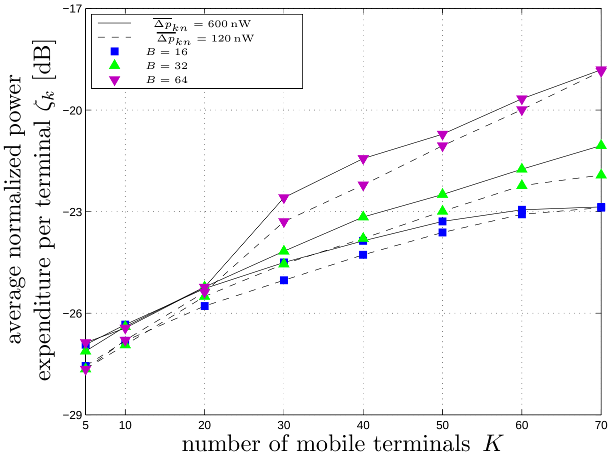

Fig. 3.6: *Average normalized power expenditure as a function of K, with $W = 10\,\mathrm{MHz}$, $N = 1024$, and $R_k^\star = R^\star = 200\,\mathrm{kb/s}$ $\forall k \in \mathcal{K}$ in the case of best-carrier assignment model.*

the schemes available in the literature (e.g., see [18, 19, 139]). Our experiments with different data rate demands show that a smaller data rate reduces also the number of operations significantly. To further reduce the number of operations, we can also increase the tolerance parameters (e.g., with $\varepsilon_2 = 0.1$, we experience a complexity reduction on the order of $20 \div 30\%$). Note also that the spectral efficiency achieved by the proposed fair resource allocation method, while showing a linear computational burden, is comparable with that provided by sum-rate maximizing algorithms (e.g., see [289]). In the practice, a reasonable value for the maximum spectral efficiency achieved by the network in the region of linear complexity in all simulated scenarios (not reported here for the sake of brevity) is slightly lower than 2 b/s/Hz. For higher spectral efficiencies, no parameter selections can achieve the optimal resource allocation with linear complexity, and the number of operations appears to increase exponentially with the number of mobile terminals. However, note that the solutions can be found in most cases.

Figs. 3.6 and 3.7 depict the simulation results of a network with $R_k^\star = R^\star = 200\,\mathrm{kb/s}$ $\forall k \in \mathcal{K}$, $N = 1024$, $W = 10\,\mathrm{MHz}$, and $\varepsilon_1 = 0, \varepsilon_2 = 0.04$ using the best-carrier assignment model. Solid lines represent the case $\overline{\Delta p}_{kn} = \overline{p}_{kn}/5 = 600\,\mathrm{nW}$, whereas dashed lines depict the case $\overline{\Delta p}_{kn} = \overline{p}_{kn}/25 = 120\,\mathrm{nW}$. Squares, upper triangles

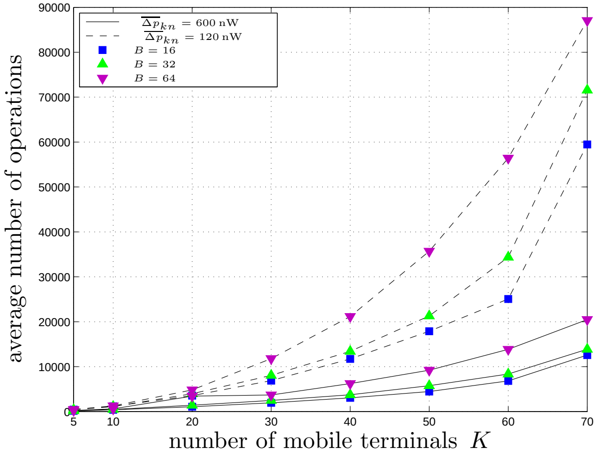

Fig. 3.7: *Experimental average number of operations as a function of K, with $W = 10\,\text{MHz}$, $N = 1024$, and $R_k^\star = R^\star = 200\,\text{kb/s}\ \forall k \in \mathcal{K}$ in the case of best-carrier assignment model.*

and lower triangles correspond to $B = \{16, 32, 64\}$, respectively. Fig. 3.6 shows the average normalized power expenditure ζ_k at the steady state as a function of K. As can be seen, the average power expenditure using the best-carrier assignment model is lower than with the vacant-carrier assignment, since the terminals having better channel conditions spend less power.

A drawback of the best-carrier assignment is an increased complexity of the algorithm. Fig. 3.7 shows the average number of operations per terminal required to reach the steady state as a function of the number of terminals K. As can be seen, the best-carrier assignment model has a computational complexity higher than vacant-carrier assignment model, since the number of shared subcarriers in the best-carrier assignment model is larger than in the vacant-carrier assignment, which increases the probability of interference between simultaneous decisions in the best-reply algorithm. Note that, using the best-carrier assignment model, the case $B = 8$ appears to be computationally expensive.

Fig. 3.8 shows the average number of operations per terminal in the case of a network with parameters $R_k^\star = R^\star = 500\,\text{kb/s}\ \forall k \in \mathcal{K}$, $N = 512$, $W = 10\,\text{MHz}$, and $\varepsilon_1 = 0, \varepsilon_2 = 0.04$ using vacant-carrier assignment model. Solid and dashed lines represents the cases $\overline{\Delta p}_{kn} = 3\,\mu\text{W}$ and $\overline{\Delta p}_{kn} = 600\,\text{nW}$, respectively, whereas circles, squares,

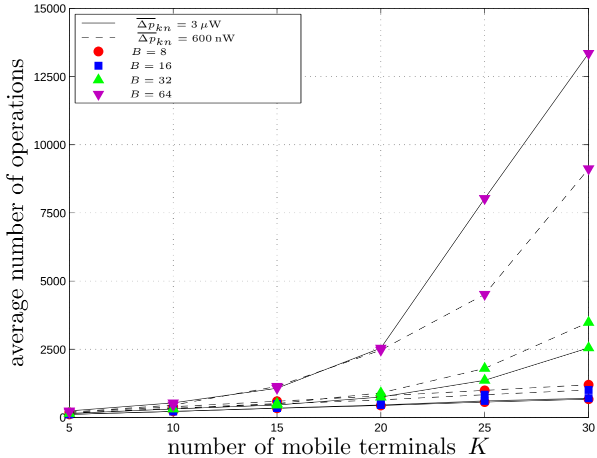

Fig. 3.8: *Experimental average number of operations as a function of* K*, with* $W = 10\,\mathrm{MHz}$*,* $N = 512$*, and* $R_k^\star = R^\star = 500\,\mathrm{kb/s}\ \forall k \in \mathcal{K}$ *in the case of vacant-carrier assignment model.*

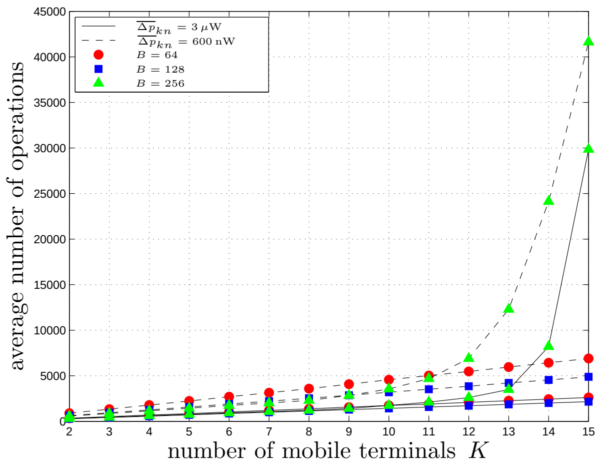

Fig. 3.9: *Experimental average number of operations as a function of* K*, with* $W = 20\,\mathrm{MHz}$*,* $N = 2048$*, and* $R_k^\star = R^\star = 2\,\mathrm{Mb/s}\ \forall k \in \mathcal{K}$ *in the case of vacant-carrier assignment model.*

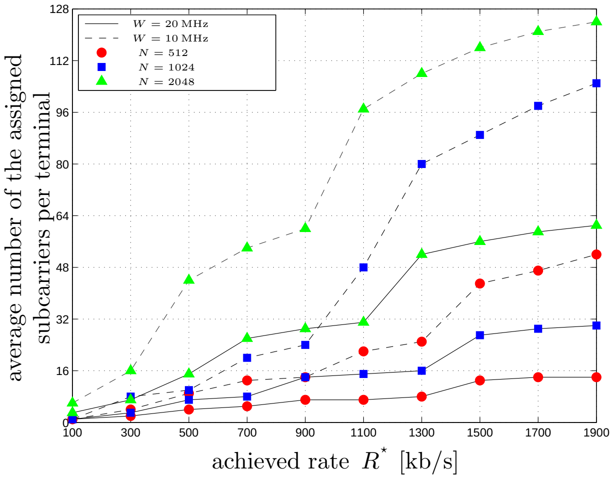

Fig. 3.10: *Average number of assigned subcarriers as a function of the achieved rate, with* $\overline{\Delta p}_{kn} = 600\,\text{nW}$ *in the case of vacant-carrier assignment model.*

upper triangles and lower triangles depict $B = \{8, 16, 32, 64\}$, respectively. Even in this case, with more severe requirements in terms of target data rates, the number of operations is shown to be *lower* than $K \cdot N$, again using spectral efficiencies higher than 1 b/s/Hz.

Finally, Fig. 3.9 shows the average number of operations per terminal in the case of a network with parameters $W = 20\,\text{MHz}$, $N = 2048$, $R_k^\star = 2\,\text{Mb/s}$, $\varepsilon_1 = 0$, and $\varepsilon_2 = 0.04$ with vacant-carrier assignment model. Solid and dashed lines represents the cases $\overline{\Delta p}_{kn} = 3\,\mu\text{W}$ and $\overline{\Delta p}_{kn} = 600\,\text{nW}$, respectively, whereas circles, squares and upper triangles depict $B = \{64, 128, 256\}$, respectively. The complexity is again *lower* than $K \cdot N$.

As can be seen in Fig. 3.5, 3.7, 3.8, and 3.9, due to the random behavior of the proposed algorithm, there is a strict relation between the average number of operations, the network parameters, and the algorithm parameters (including the channel assignment model). Depending on the parameter selection, we see different shapes (linear or exponential behavior) for the average number of operations. Thus, estimating the analytical complexity function for the best-response algorithm is hard to do. However, for *all* tested scenarios (not reported here for the sake of brevity), there exist properly tuned values (such as $B, \overline{\Delta p}_{kn}$) that provide an average number of operations for the proposed algorithm that are *lower* than the product $K \cdot N$, even with high data rate demands like in the cases of Figs. 3.8 and 3.9. The parameter that most impacts on the number of operations is B. Our experiments show that, for the optimal parameter selection (i.e., when the number of operations scales linearly with N and K), the average number of used subcarriers per terminal (i.e., those which bear $p_{kn} > 0$) is approximately $B/2$ when the vacant-carrier model is adopted. This rule-of-thumb can be used as a design criterion for the proposed algorithm. Let us consider Fig. 3.10, that reports the average number of assigned subcarriers to each mobile terminal as a function of the achieved rate $R^{\star}$, in the linear complexity regime and using $\overline{\Delta p}_{kn} = 600\,\text{nW}$. Dashed and solid lines depict the cases $W = \{10, 20\}\,\text{MHz}$, respectively, whereas circles, squares and upper triangles represent $N = \{512, 1024, 2048\}$, respectively. For instance, when $W = 20\,\text{MHz}$, $N = 512$, and $R^{\star} = 500\,\text{kb/s}$, the average number of used subcarriers is 4. If we look back at Fig. 3.8, we can verify that the linear complexity can be achieved using $B = 8$. Note that the number of assigned subcarriers in the case of $W = 10\,\text{MHz}$ is higher than in the case $W = 20\,\text{MHz}$, since the subcarrier spacing is halved.

3.4 Discussion

This chapter described a computationally inexpensive centralized algorithm based on coalitional game theory to address the issue of fair optimal resource allocation (in terms of subcarrier assignment and power control) for the uplink of an infrastructure OFDMA wireless network. The scheme derived here is designed to meet the required data rates exactly, thus ensuring a fair performance apportionment to both users and service providers, with the best utilization of the network resources (minimum power expenditure and good spectral efficiency). The proposed algorithm can be analyzed as a Markov model that converges to an absorbing state with unitary probability in the long run. Our criterion also allows us to tradeoff system performance and computational burden of the algorithm, based on the number of subblocks used to apportion the available bandwidth and the data rate requirements of the terminals. Simulations show that the target rates are achieved with a low complexity procedure, even in the case of populated networks and stringent QoS requirements. The (greedy) best-carrier assignment rule results into a higher complexity but a lower power expenditure compared to the case with full use of the available subcarriers. The presented coalition-based strategy appears to be a good tradeoff between computational complexity and power efficiency in comparison with the schemes available in the literature, and achieves a spectral efficiency larger than 1 b/s/Hz.